Structure and Bonding of the Noble Gas−Metal Carbonyl Complexes $M(CO)_5$−Ng (M = Cr, Mo, W and Ng = Ar, Kr, Xe)

Andreas W. Ehlers,*,† Gernot Frenking,‡ and Evert Jan Baerends†

Afdeling Theoretische Chemie, Scheikundig Laboratorium der Vrije Universiteit, De Boelelaan 1083, NL-1081 HV Amsterdam, The Netherlands, and Fachbereich Chemie, Philipps-Universität Marburg, Hans-Meerweinstrasse, D-35032 Marburg, Germany

Received June 11, 1997[⊗]

Quantum mechanical ab initio calculations at the MP2 and CCSD(T) level of theory using effective core potentials for the heavy atoms as well as density functional calculations using various gradient corrections are reported for the noble gas−transition metal pentacarbonyl complexes $M(CO)_5$−Ng (M = Cr, Mo, W and Ng = Ar, Kr, Xe). The optimized geometries show increasing metal−noble gas distances in the order Ar < Kr < Xe and Cr < W < Mo. The theoretically predicted M−Ng bond energies are very close to experimentally observed data. The nature of the interactions between the unsatured 16 e^- fragments $M(CO)_5$ and the noble gases is investigated using the topological analysis of the electron density distribution and by a detailed analysis of the bond energies. Excitation energies are predicted using time-dependent density functional theory in good agreement with experimental measurements.

Introduction

In 1975, Perutz and Turner made the observation that the position of the visible band in the UV spectra of the matrix-generated pentacarbonyls $M(CO)_5$ (M = Cr, Mo, W) is extraordinarily sensitive to the matrix material, for which, among others, the "inert" gases Ne, Ar, Kr, and Xe were used.[1] The experimental findings were interpreted by assuming that $M(CO)_5$, forms a weak bond with the noble gas (Ng) atoms.[1] Subsequent work by the same authors reported the FTIR spectra of Cr-$(CO)_5$−Xe in liquid Xe and Kr, providing further evidence for the formation of noble gas complexes with remarkable stability.[2,3] More recently, Wells and Weitz were able to report the $(OC)_5$M−Xe bond dissociation energy for M = Cr (9.0 ± 0.9 kcal/mol), Mo (8.0 ± 1.0 kcal/mol, and W (8.2 ± 1.0 kcal/mol), by measuring the temperature dependence of the dissociation rate constant in the gas phase.[4] The same workers estimated upper limits for the $(OC)_5$W−Kr bond (<6 kcal/mol) and the $(OC)_5$W−Ar bond (≤3 kcal/mol).[4] The same technique applied in liquid xenon by Weiller gave a bond energy of 8.4 ± 0.2 kcal/mol, in excellent agreement with the gas-phase value.[5] In a very recent study by Sun et al.[6] of the decay of $M(CO)_5$−Ng in supercritical CO_2 and noble gas fluids by time-resolved IR techniques the activation energy of 8.2 ± 0.2 kcal/mol for $(OC)_5$W−Xe was obtained, which is identical to the W-Xe bond strength measured by Wells and Weitz. Furthermore it was confirmed that the reactivity of the tungsten pentacarbonyl noble gas complexes decreases in the order Ar > Kr > Xe. The reactivity of $(OC)_5$M-Xe and $(OC)_5$M−Kr was found to be Cr ≈ Mo > W.

The experimental studies of the $M(CO)_5$-Ng complexes provide information about the infrared spectra and bond energies of these unusual molecules. No information about the bond lengths and the nature of the metal−noble gas bonds is given. In principle, this information could be given by quantum mechanical methods. The only theoretical study of the complexes has been published by Demuynck et al.,[7] who reported ab initio calculations at the SCF level of $M(CO)_5$−Ng (M = Cr, Mo; Ng = Ar, Kr, Xe). Due to the limited computational resources available at that time, the study can only be considered as qualitative. At present, there are two theoretical methods available that can handle the huge computational effort needed for these systems due to the large number of electrons of the heavy atoms and the relativistic effects that have to be taken into account. These are based on either density functional theory (DFT) or on effective core potentials (ECP). We have recently shown that the geometries and metal−ligand bond energies of $M(CO)_5$−L (M = Cr, Mo, W; L = CO, CS, SiO, N_2, CN^-, NC^- NO^+) are predicted with good accuracy at the CCSD(T)/II//MP2/II level of theory, where II denotes a 6-3lG(d) basis set for the ligands and an ECP with a DZ+P quality valence basis set for the metals.[8−10] Also the metal−ligand bond energies of the more weakly bound dihydrogen ligand in $M(CO)_5$−H_2 are predicted in excellent agreement with experiment.[11] The calculated value for $Cr(CO)_5$−H_2 was D_o = 15.9

† Scheikundig Laboratorium der Vrije Universiteit.
‡ Philipps-Universität Marburg.
[⊗] Abstract published in *Advance ACS Abstracts,* October 1, 1997.

(1) Perutz, N. R.; Turner, J. J. *J. Am. Chem. Soc.* **1975**, *97*, 4791.
(2) Burdett, J. K.; Grzybowsky, J. M.; Perutz, R. N.; Poliakoff, M.; Turner, J. J.; Turner, R. F. *Inorg. Chem.* **1978**, *17*, 147.
(3) Turner, J. J.; Burdett, J. K.; Perutz, R. N.; Poliakoff, M. *Pure Appl. Chem.* **1977**, *49*, 271.
(4) Wells, J. R.; Weitz, E. *J. Am. Chem. Soc.* **1992**, *114*, 2783.
(5) Weiller, B. H. *J. Am. Chem. Soc.* **1992**, *114*, 10910.
(6) Sun, X.; George, M. W.; Kazarian, S. G.; Nikiforov, S. M.; Poliakoff, M. *J. Am. Chem. Soc.* **1996**, *118*, 10525.
(7) Demuynck, J.; Kochanski, E.; Veillard, A. *J. Am. Chem. Soc.* **1979**, *101*, 3467.
(8) Ehlers, A. W.; Frenking, G. *J. Chem. Soc., Chem. Commun.* **1993**, 1709.
(9) Ehlers, A. W.; Frenking, G. *J. Am. Chem. Soc.* **1994**, *116*, 1514.
(10) Frenking, G.; Antes, I.; Böhme, M.; Dapprich, S.; Ehlers, A. W.; Otto, R.; Stegmann, R.; Veldkamp, A.; Vyboishchikov, S. F. in *Reviews in Computational Chemistry*; Lipkowitz, K. B., Boyd, D. B., Eds.; VCH Publishers: New York, 1996; Vol. 8, p 63.
(11) Dapprich, S.; Frenking, G. *Angew. Chem.* **1995**, *107*, 383; *Angew. Chem., Int Ed. Engl.* **1995**, *34*, 354.

S0276-7333(97)00496-2 CCC: $14.00

kcal/mol; the experimental value is 15.0 + 1.3 kcal/mol.[12] This shows that the ECP methods used by us for the calculation of transition metal complexes give accurate bond energies even for weakly bound ligands.

It has been proven that results of DFT-based methods using gradient-corrected functionals (the generalized gradient approximation, GGA) are comparable to those of classical ab initio methods for calculations of transition metal complexes with strongly bound ligands. The geometries of the first-row transition metal complexes are predicted in even better agreement with experimental values by density functional theory than at the MP2 level, and the calculated bond dissociation energies are very close to the CCSD(T) values.[13−15] However, it has been reported that GGA methods can fail for the calculation of weak interactions such as van der Waals forces between noble gas diatomics.[16]

Here we report theoretically predicted geometries and bond energies of the title compounds. The performance of different gradient approximations is compared to high-level ab initio techniques. The nature of the metal−noble gas bond is examined using the topological analysis of the MP2 electron density distribution.[17] The dependence of the excitation energies on the noble gas atoms is examined by time-dependent density functional theory (TDDFT).[18−21]

Methods

The geometries of the complexes have been optimized at the MP2 level of theory[22,23] using ECPs for the metals and 6-31G(d) all-electron basis sets for C and O.[24] The small-core ECPs of Hay and Wadt[25] include the $(n - 1)s^2$ and $(n - 1)p^6$ electrons as part or the valence electrons, for which a [441/2111/*N*-11] (N = 5, 4, 3 for Cr, Mo, W, respectively) valence basis set is chosen. The ECPs for the noble gases are taken from Stoll and Preuss.[26,27] The valence basis sets for Ar, Kr, and Xe are [3111/3111/1]. This basis set combination is our standard basis II.[10] The most important relativistic effects are included in the ECPs of the noble gases, Mo and W. The ECP for Cr is nonrelativistic.[25] It has been shown that relativistic and nonrelativistic ECPs give nearly the same results for chromium carbonyl complexes.[8,9] Improved dissociation energies are calculated at the CCSD(T) level[28] using the same basis sets at the MP2-optimized geometries. For the calculation of the correlation energy, the 1s orbitals of carbon and oxygen were kept frozen. The zero-point energy corrections are predicted at the HF level. For the geometry optimization, the program Gaussian 92[29] was used. The CCSD(T) calculations were carried out using the program Aces II.[30]

The DFT-based calculations reported in this paper have been carried out by using the new parallel version of the Amsterdam Density Functional (ADF)[31−33] program. The frozen core approximation[34] was applied in such a way that the valence space was identical to the ECP calculations. The frozen core orbitals have been taken from atomic calculations in a very large basis set. To make the valence orbitals orthogonal to the cores, the valence basis sets have been augmented with a single-ζ STO for each atomic core orbital.

The MOs of the transition metals and noble gases are expanded in a large basis set of Slater-type orbitals (STOs) of triple-ζ quality with three STOs per nl shell.[35,36] For carbon and oxygen, a quadruple-ζ STO basis set was used.[14] We added one p STO to the transition metals and one d STO for the main group as polarization functions. One additional f polarization function and two s, two p, and two d diffuse functions were added to the noble gas basis sets. This basis set combination will be referred in the following as basis III.

The present investigation makes full use of the self-consistent implementation of the density gradient (or nonlocal) corrections in the geometry optimization as well as energy calculation[37] including scalar relativistic effects.[38−42] For the energy calculations the local exchange-correlation potential parametrized by Vosko, Wilk and Nusair[43] is used in combination with two different GGAs. These nonlocal corrections were based on Becke's functional for exchange[44] in combination with Perdew's functional for correlation[45] (BP86) or alternatively on the revised general gradient approximation by Perdew and Wang (PW91)[46] for both exchange and correlation.

Results and Discussion

Table 1 shows the optimized geometries of $M(CO)_5$-Ng complexes and the $M(CO)_5$ fragments predicted at the BP86 level of theory using basis set combination III. The most interesting aspect of the calculated data concerns the bond angle between the axial and equatorial CO groups α (Figure 1).

(12) Wells, J. R.; House, P. G.; Weitz, E. *J. Phys. Chem.* **1994**, *98*, 8343.
(13) Ziegler, T. *Can. J. Chem.* **1995**, *73*, 743.
(14) Rosa, A.; Ehlers, A. W.; Baerends, E. J.; Snijders, J. G.; Velde, G. t. *J. Phys. Chem.* **1996**, *100*, 5690.
(15) Li, J.; Schreckenbach, G.; Ziegler, T. *J. Am. Chem. Soc.* **1995**, *117*, 486.
(16) Pérez-Jordá, J.; Becke, A. D. *Chem. Phys. Lett.* **1995**, *233*, 134.
(17) Bader, R. F. W. *Atoms in Molecules. A Quantum Theory*; Oxford Press: New York, 1990.
(18) Casida, M. E. In *Recent Advances in Density Functional Methods*; Chong, D. P., Ed.; World Scientific: Singapore, 1995; p 155.
(19) Bauernschmitt, R.; Ahlrichs, R. *Chem. Phys. Lett.* **1996**, *256*, 454.
(20) Bauernschmitt, R.; Ahlrichs, R. *Chem. Phys. Lett.* **1997**, *264*, 573.
(21) Kootstra, F. Internal report, Free University of Amsterdam, The Netherlands, 1997.
(22) Møller, C.; Plesset, M. S. *Phys. Rev.* **1934**, *46*, 618.
(23) Binkley, J. S.; Pople, J. A. *Int. J. Quantum Chem.* **1975**, *9*, 229.
(24) Ditchfield, R.; Hehre, W. J.; Pople, J. A. *J. Chem. Phys.* **1971**, *54*, 724.
(25) Hay, P. J.; Wadt, W. R. *J. Chem. Phys.* **1985**, *82*, 299.
(26) Nicklass, A.; Dolg, M.; Stoll, H.; Preuss, H. manuscript in preparation.
(27) Nicklass, A.; Dolg, M.; Stoll, H.; Preuss, H. Diplom Thesis, Stuttgart, 1990.
(28) Pople, J. A.; Head-Gordon, M.; Raghavachari, K. *J. Chem. Phys.* **1987**, *87*, 5968.
(29) Frisch, M. J.; Trucks, G. W.; Head-Gordon, M.; Gill, P. M. W.; Wong, M. W.; Foresman, J. B.; Johnson, B. G.; Schlegel, H. B.; Robb, M. A.; Replogle, E. S.; Gomberts, R.; Andreas, J. L.; Raghavachari, K.; Binkley, J. S.; Gonzales, C.; Martin, R. L.; Fox, D. J.; Defrees, D. J.; Baker, J.; Stewart, J. J. P.; Pople, J. A. Gaussian Inc., Pittsburgh, PA, 1992.
(30) Stanton, J. F.; Gauss, J.; Watts, J. D.; Lauderdale, W. J.; Bartlett, R. J. University of Florida, Gainsville, FL, 1991.
(31) Guerra, C. F.; Visser, O.; Snijders, J. G.; Velde, G. t.; Baerends, E. J. In *METECC-95*; Clementi, E., Corongiu, C., Eds.; Cagliari: 1995; p 307.
(32) Baerends, E. J.; Ros, P. *Chem. Phys.* **1973**, *2*, 52.
(33) Velde, G. t.; Baerends, E. J. *J. Comput. Phys.* **1992**, *99*, 84.
(34) Baerends, E. J.; Ellis, D. E.; Ros, P. *Chem. Phys.* **1973**, *2*, 41.
(35) Snijders, J. G.; Baerends, E. J.; Vernooijs, P. *At. Nucl. Data Tables* **1982**, *26*, 483.
(36) Vernooijs, P.; Snijders, J. G.; Baerends, E. J. Internal report, Free University of Amsterdam, The Netherlands, 1981.
(37) Fan, L.; Versluis, L.; Ziegler, T.; Baerends, E. J.; Ravenek, W. *Int. J. Quantum. Chem., Quantum Chem. Symp.* **1988**, *S22*, 173.
(38) Pyykkö, P. *Chem. Rev.* **1988**, *88*, 563.
(39) Snijders, J. G.; Baerends, E. J. *Mol. Phys.* **1978** *36*, 1789.
(40) Snijders, J. G.; Baerends, E. J.; Ros, P. *Mol. Phys.* **1979**, *38*, 1909.
(41) Ziegler, T.; Tschinke, V.; Baerends, E. J.; Snijders, J. G.; Ravenek, W. *J. Phys. Chem.* **1989**, *93*, 3050.
(42) Boerrigter, P. M. Spectroscopy and Bonding of heavy element compounds. Ph.D. Thesis, Vrije Universiteit, Amsterdam, The Netherlands, 1987.
(43) Vosko, S. H.; Wilk, L.; Nusair, M. *Can. J. Phys.* **1980**, *58*, 1200.
(44) Becke, A. D. *Phys. Rev. A* **1988**, *38*, 3098.
(45) Perdew, J. P. *Phys. Rev. B* **1986**, *33*, 8822.
(46) Perdew, J. P.; Wang, Y. *Phys. Rev. B* **1992**, *46*, 6671.

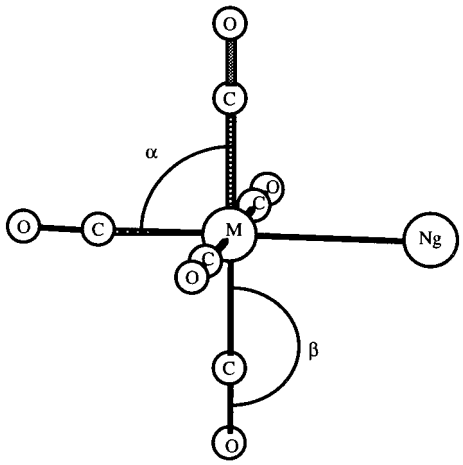

Figure 1. Definition of the bond angles α and *β*.

Table 1. Bond Lengths (Å) and Angles (deg) Using [BP(86)/III]

	M−C_{eq}	C−O_{eq}	M−C_{ax}	C−O_{ax}	M−NG	α	*β*
$Cr(CO)_5Ar$	1.898	1.158	1.824	1.163	2.742	89.5	177.2
$Cr(CO)_5Kr$	1.900	1.158	1.830	1.163	2.870	90.3	178.5
$Cr(CO)_5Xe$	1.897	1.158	1.831	1.164	2.994	89.6	177.4
$Cr(CO)_5$	1.902	1.158	1.826	1.164		90.3	177.4
$Mo(CO)_5Ar$	2.056	1.158	1.956	1.165	2.860	90.2	179.2
$Mo(CO)_5Kr$	2.053	1.158	1.959	1.165	2.944	90.1	179.1
$Mo(CO)_5Xe$	2.055	1.158	1.964	1.165	3.095	89.8	178.7
$Mo(CO)_5$	2.055	1.157	1.944	1.165		89.8	178.1
$W(CO)_5Ar$	2.058	1.159	1.962	1.166	2.852	90.6	179.3
$W(CO)_5Kr$	2.052	1.160	1.971	1.167	2.933	89.9	178.8
$W(CO)_5Xe$	2.048	1.161	1.972	1.167	3.060	89.6	178.3
$W(CO)_5$	2.056	1.159	1.956	1.167		90.2	178.5

The bond angle α has been very important for the interpretation of the UV spectra of the metal carbonyls in noble gas matrixes by Turner et al.[1−3] They estimated α to be 91.3° for $Cr(CO)_5$-Xe and 95.5° for $Cr(CO)_5$-Ar based on the relative intensities of metal carbonyl bands in IR spectra. The major visible transition of the species is due to the $e \rightarrow a_1$ transition.[1−3,47,48] The shift of the visible bands toward lower wavenumbers from $Cr(CO)_5$-Xe to $Cr(CO)_5$−Ne was explained by the lowering of the energy difference between the HOMO (e) and the LUMO (a_1). Because the energy level of the a_1 LUMO decreases sharply[2,3,49] from α = 60° to α = 120° (the e HOMO has a minimum at 90°), the trend in the IR spectra was taken as evidence that α increases from $Cr(CO)_5$-Xe to $Cr(CO)_5$-Ar. The SCF calculations by Demuynck et al.[7] predict values of 92° for $Cr(CO)_5$ and 9l° for $Mo(CO)_5$.

The theoretical results from Table 1 indicate that α is about 90° in the pentacarbonyls. The geometries of the pentacarbonyl fragments are almost unchanged when the complex with the noble gas is formed. Especially the variation of α due to complexation to Ar, Kr, or Xe is negligible, and the differences are too small (<1°) to explain the band shift observed in the UV spectra.

There is a small lengthening of the metal−carbonyl bond, which is in trans position to the noble gas. This lengthening is the largest for $W(CO)_5$-Xe with 0.02 Å. The shortest metal−Ng distance is found for $Cr(CO)_5$-Ar with a value of 2.74 Å. The metal−Ng bond length increases in the order Ar < Kr < Xe by about 0.1 Å. The Mo-Ng bonds are significantly longer than the respective Cr-Ng bonds, while the W-Ng bonds are slightly shorter than Mo-Ng. This is analogous to the trend of the metal−carbonyl bond distances. The revised general gradient approximation by Perdew and Wang (PW91) and the ab initio calculations predict structural parameters that are very close to those calculated with BP86 and are therefore not shown in Table 1. The largest differences are observed for the chromium compounds, where the Cr−CO and Cr-Ng bond lengths are predicted to be longer than found using MP2/II. This is in agreement with earlier theoretical studies on the transition metal hexacarbonyls. It is well-known that MP2 predicts too short metal−carbonyl bond distances for first-row transition metals.[13,15] Generally, DFT methods are more reliable than HF-based ab initio methods for compounds of first-row transition metals with a partially filled d shell.[10]

Table 2. Calculated and Experimental Polarizabilities of the Noble Gas Atoms (10^{-24} cm^3)

method	basis set	Ar	Kr	Xe
HF	II	0.716	1.086	2.352
MP2	II	0.723	1.064	2.340
CCSD(T)	CCSD(T)/II-SP	0.730	1.068	2.364
HF	II + $W(CO)_5$ ghost functions	1.254	2.019	3.388
BP86	III	1.737	2.597	4.188
PW91	III	1.787	2.666	4.250
exp	exp	1.64	2.48	4.04

The metal−Ng bond is to some extent due to dipole-induced dipole interactions. In order to estimate the reliability of the calculated attractive interactions between the $M(CO)_5$ fragments and the noble gas atoms, we calculated the electric polarizabilities of Ar, Kr, and Xe at different theoretical levels. The results are shown in Table 2. The theoretical values at the HF level using the valence basis sets II of the Ng atoms are only half of the experimental data. The correlation contribution to the calculated polarizabilities using this basis set is negligible. However, the contribution by the basis set superposition of the $M(CO)_5$ fragments to the calculated polarizability is very large, indicating the restricted nature of basis II. The theoretically predicted electric polarizabilities calculated with inclusion of the ghost functions are 75−80% of the experimental values. Thus, the calculations should recover most of the dipole-induced dipole interactions. The theoretical values of the DFT-based calculations of the electric polarizabilities using the large STO basis set III are very close to the experiment. The values are about 5−10% overestimated. The differences to the experimental values are somewhat smaller for the GGA of Becke and Perdew (BP86) than those of Perdew and Wang (PW91). Addition of the ghost functions does not change the values significantly, indicating the good quality of the STO basis set III.

Table 3 shows the theoretically predicted and experimentally observed bond energies. Since the experimental values are based on rated constants measured at T = 298 K, we converted the directly calculated dissociation energies ΔE into the bond enthalpies ΔH_{298}. The thermal corrections for reaction (1) include the work term $pV = RT$ (0.6 kcal/mol) and three degrees of translation (0.9 kcal/mol). ZPE corrections are also added, although they are negligible (<0.2 kcal/mol).

(47) Cotton, F. A.; Edwards, W. T.; Rauch, F. C.; Graham, M. A.; Perutz, N. R.; Turner, J. J. *J. Coord. Chem* **1973**, *2*, 247.
(48) Wrighton, M. *Inorg. Chem.* **1974**, *13*, 905.
(49) Elian, M.; Hoffman, R. *Inorg. Chem.* **1975**, *14*, 1058.

Table 3. Dissociation Energies (kcal/mol) $M(CO)_5$−Ng M = Cr, Mo, W, and Ng = Ar, Kr, Xe

	CCSD(T)/II			BP86/III			PW91/III			
	ΔE	ΔH_{298}	ΔH_{298} BSSE corr.	ΔE	ΔH_{298}	ΔH_{298} BSSE corr.	ΔE	ΔH_{298}	ΔH_{298} BSSE corr.	exp ΔH_{298}
$Cr(CO)_5Ar$	4.9	6.3	3.5	1.9	3.3	3.0	3.8	5.2	4.8	
$Cr(CO)_5Kr$	6.2	7.5	4.7	3.0	4.3	4.0	5.0	6.3	5.9	
$Cr(CO)_5Xe$	7.2	8.5	5.0	5.4	6.7	6.4	7.6	8.9	8.5	9.0 ± 0.9
$Mo(CO)_5Ar$	5.4	6.8	2.2	2.7	4.1	3.6	4.0	5.4	4.9	
$Mo(CO)_5Kr$	6.9	8.2	4.4	3.9	5.2	4.7	5.1	6.4	5.9	
$Mo(CO)_5Xe$	8.2	9.5	4.7	7.0	8.3	7.9	8.6	9.9	9.4	8.0 ± 1.0
$W(CO)_5Ar$	8.0	9.4	4.3	3.6	5.0	4.6	5.2	6.6	6.1	$\leq\sim 3$
$W(CO)_5Kr$	10.0	11.3	6.7	5.1	6.4	6.0	7.0	8.3	7.8	≤ 6
$W(CO)_5Xe$	11.9	13.2	7.6	7.6	8.9	8.8	9.8	11.1	10.7	8.2 ± 1.0

$$M(CO)_5{-}Ng \rightarrow M(CO)_5 + Ng \qquad (1)$$

The calculated dissociation energies at the CCSD(T) level of theory using basis set combination II for Cr-$(CO)_5$-Xe (ΔH_{298} = 8.5 kcal/mol), Mo$(CO)_5$-Xe (ΔH_{298} = 9.5 kcal/mol), and W$(CO)_5$-Xe (ΔH_{298} = 13.2 kcal/mol) are too high compared to the experimental values. The medium-sized basis set II will cause a substantial basis set superposition error (BSSE) . In previous studies of more strongly bound transition metal complexes, we did not correct for the BSSE, because we argued that the BSSE contribution roughly cancels the error due to the basis set incompletion.[9−11,50,51] However, this may not be justified for weakly bound systems, where the BSSE may lead to a substantial overestimation of the bond energy.[52] For this reason we corrected the $(OC)_5$M-Ng bond energies for the BSSE using the counter poise correction.[14,53]

Table 3 shows that the BSSE-corrected CCSD(T)/II bond energies are substantially lower than the uncorrected values. The BSSE is between 2.8 (Cr$(CO)_5$-Kr) and 5.6 kcal/mol (W$(CO)_5$-Xe). The BSSE-corrected bond energy of W$(CO)_5$-Xe (ΔH_{298} = 7.6 kcal/mol) is slightly lower than the experimental values of 8.2 ± 1.0 and 8.4 ± 0.2 kcal/mol. This is reasonable, because the calculated polarizabilities of the noble gases are slightly too small. Also, the corrected bond energies for W$(CO)_5$-Kr (ΔH_{298} = 6.7 kcal/mol) and W$(CO)_5$-Ar (ΔH_{298} = 4.3 kcal/mol) are in reasonable agreement with the experimental estimate. A difference between theory and experiment is found for the bond energies calculated at CCSD(T) for Mo$(CO)_5$-Xe and Cr$(CO)_5$-Xe. The calculations predict that the Mo−Xe and Cr-Xe bonds are clearly weaker by ~3 kcal/mol than the W-Xe bond. The experimental values measured by Wells and Weitz[4] indicate that the three metal−xenon bonds should have practically the same strength. However, the most recent investigation by Sun et al.[6] of the decay of $M(CO)_5$-Ng showed that the reactivity is Cr ≈ Mo > W, which supports the theoretically predicted trend. Please note that the BSSE-corrected bond energies at CCSD(T) now give a trend of increasing bond strength for the metals Mo < Cr < W. Since bond energies of first-row transition metals are calculated too short and too strong by HF-based methods,[10] the bond energies for the Cr-Ng bonds are probably slightly too high.

The differences to the experimental values are probably caused by the insufficient basis set, but this error should be equal for the three metals. However, the use of the computationally costly CCSD(T) method limited the size of the valence basis set, that could be used. Therefore, we used the DFT approach for the calculations with the extended basis set III. The BSSE for this basis set is very low with values of 0.3−0.5 kcal/mol when the gradient corrections of BP86 are applied and 0.5−0.6 kcal/mol for the PW91 corrections. The bond dissociation energies predicted at BP86/III are in excellent agreement with the corrected CCSD(T) values, with the notable exception of Mo$(CO)_5$−Xe, which appears to be too low at CCSD(T). The metal−Xe bond strengths are predicted to be slightly higher and the metal−Ar, and metal−Kr bonds are almost identical. The largest bond enthalpies are calculated using the revised gradient corrections of PW91. Those values are in general ~2 kcal/mol higher, and the agreement with the other methods is still very good. The results based on density functional theory give the trend of increasing bond dissociation energies for Cr < Mo < W. The trend of the bond energies for the noble gas atoms is correctly predicted at all levels of theory Ar < Kr < Xe.

We examined the nature of the metal−Ng bonds using the topological analysis of the electron density distribution and its associated gradients and Laplacian[17] of the MP2 wave functions. Figure 2 shows the Laplacian distribution of W$(CO)_5$-Xe in the plane containing the Xe atom and two equatorial carbonyl groups. The area of electron concentration ($\nabla^2\rho(r) < 0$, solid lines) in the valence sphere of xenon exhibits a nearly perfect round shape, which indicates that the electronic structure of Xe is hardly disturbed in the complex. The Laplacian distribution of the other $M(CO)_5$-Ng complexes is very similar. Therefore, it is not shown here. It is instructive to compare the W-Xe bond of W$(CO)_5$-Xe with the Xe−BeO bond in XeBeO.[54] The Laplacian distribution of the latter is shown in Figure 3. The difference is striking. There is a clear deformation of the area of charge concentration around Xe in XeBeO, which indicates the onset of a covalent bond.

The energy density at the bond critical points H_b of the metal−Ng bonds is clearly different to the energy density of the donor−acceptor-type interactions of the metal−carbonyl bonds. The donor−acceptor-type M−CO bonds have typical H_b values between 0.2 and 0.7 hartree Å^{-3}. However, the energy density in the bond critical points of the metal−noble gas bonds are almost zero. It has been shown that covalent bonds have negative H_b values, while ionic and closed-shell interactions are characterized by $H_b \sim 0$.[56] The $(OC)_5$W-Xe bond has a value H_b = −0.011 hartree Å^{-3}, which is

(50) Ehlers, A.; Frenking, G. *Organometallics* **1995**, *14*, 423.
(51) Ehlers, A. W.; Dapprich, S.; Vyboishchikov, S. F.; Frenking, G. *Organometallics* **1996**, *15*, 105.
(52) Lenthe, J. H. v.; Rijdt, J. G. C. v D.-v Duijneveldt, F. B. v. *Ab initio Methods in Quantum Chemistry*; John Wiley and Sons: New York, 1987; Part II, Vol. LXIX.
(53) Boys, S. F.; Bernardi, F. *Mol. Phys.* **1979**, *37*, 1529.
(54) Veldkamp, A.; Frenking, G. *Chem. Phys. Lett.* **1994**, *226*, 11.
(55) Cioslowsky, J.; Mixon, S. T. *J. Am. Chem. Soc.* **1991**, *113*, 4142.

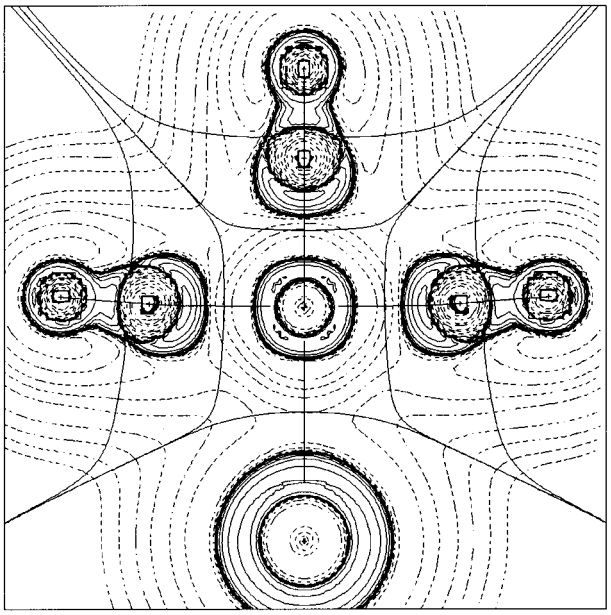

Figure 2. Contour line diagram of the Laplacian distribution $\nabla^2\rho(r)$ of $W(CO)_5$−Xe. Dashed lines indicate charge depletion ($\nabla^2\rho(r) > 0$); solid lines indicate charge concentarion ($\nabla^2\rho(r) < 0$). The solid lines connecting nuclei are the bond paths; the solid lines separating the atomic nuclei indicate the zero-flux surfaces in the molecular plane. The crossing points of the bond paths and the zero-flux surfaces are the bond critical points r_b.

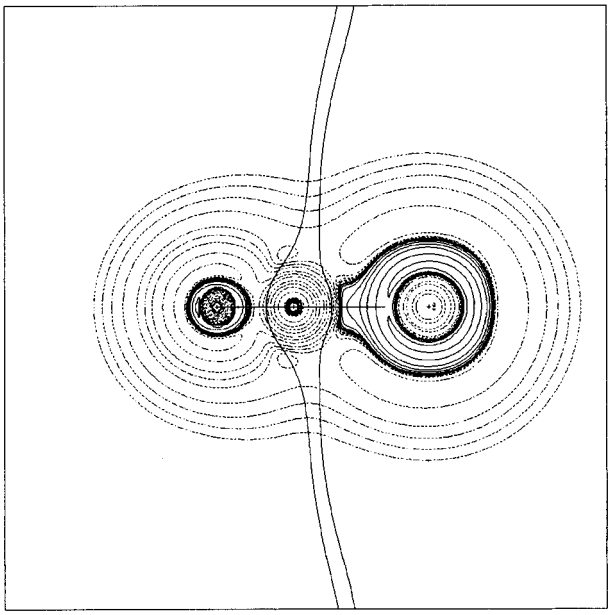

Figure 3. Contour line diagram of the Laplacian distribution $\nabla^2\rho(r)$ of XeBeO. Dashed lines indicate charge depletion ($\nabla^2\rho(r) > 0$); solid lines indicate charge concentarion ($\nabla^2\rho(r) < 0$). The solid lines connecting the atomic the atomic nuclei are the bond paths; the solid lines separating the atomic nuclei indicate the zero-flux surfaces in the molecular plane. The crossing points of the bond paths and the zero-flux surfaces are the bond critical points r_b.

the most negative value of the $M(CO)_5$-Ng complexes investigated here. The H_b of the Xe−BeO bond is −0.033 hartree Å^{-3}; the bond strength is calculated as D_o = 14.7 kcal/mol. XeBeO has recently been observed experimentally.[57] The calculated bond orders[55] of the M-Ng bonds are rather small with values between 0.2 and 0.3. However, the bond order increase in the row Ar < Kr < Xe and in the row Cr < Mo < W corresponds to the trend of the bond dissociation energies.

Table 4. Results of the Bond Energy Analysis Using [BP(86)/III] (kcal/mol)

	$Cr(CO)_5Ar$	$Cr(CO)_5Kr$	$Cr(CO)_5Xe$
ΔE_{Pauli}	10.2	12.1	16.3
ΔE_{Elstat}	−4.8	−6.2	−9.0
$\Delta E_{oi}(A_1)$	−5.5	−7.0	−10.1
$\Delta E_{oi}(E)$	−1.8	−1.9	−2.5
	$Mo(CO)_5Ar$	$Mo(CO)_5Kr$	$Mo(CO)_5Xe$
ΔE_{Pauli}	10.1	13.3	16.4
ΔE_{Elstat}	−4.8	−6.9	−9.4
$\Delta E_{oi}(A_1)$	−5.6	−7.4	−9.9
$\Delta E_{oi}(E)$	−2.1	−2.4	−2.9
	$W(CO)_5Ar$	$W(CO)_5Kr$	$W(CO)_5Xe$
ΔE_{Pauli}	11.9	15.5	20.8
ΔE_{Elstat}	−6.1	−8.7	−12.5
$\Delta E_{oi}(A_1)$	−6.9	−9.0	−12.0
$\Delta E_{oi}(E)$	−2.1	−2.4	−3.0

In order to investigate the closed-shell interaction in more detail, we performed a bond energy analysis using the fragment-based decomposition scheme implemented in ADF. The bond dissociation energy (BDE) is split into the preparation energy ΔE_{prep}, which is the energy difference the two $M(CO)_5$ fragments possess in their equilibrium geometry and in the geometry of the complex, and the interaction energy ΔE_{int}, which is the energy change when the two fragments are combined together.

$$-\mathrm{BDE} = \Delta E_{prep} + \Delta E_{int}$$

The interaction energy ΔE_{int} is made up of the usually attractive electrostatic interaction ΔE_{elst} between the unperturbed charge distributions of the fragments in the complex geometry, the Pauli repulsion ΔE_{Pauli}, which represents the four-electron interaction between the occupied orbitals, and the orbital interaction ΔE_{oi}. ΔE_{oi} describes the charge transfer in the case of interaction between occupied orbitals of one fragment and the virtual orbitals of the other fragment and the polarization in the case of mixing occupied and empty orbitals of the same fragment.

$$\Delta E_{int} = \Delta E_{Elstat} + \Delta E_{Pauli} + \Delta E_{oi}$$

Symmetry partitioning of the orbital interaction yields the contributions of each irreducible representation.

$$\Delta E_{oi} = \sum_{\Gamma} \Delta E_{\Gamma}$$

The results of the bond energy decomposition calculated with BP/III are shown in Table 4. The preparation energy ΔE_{prep} needed to change the geometry of the pentacarbonyls from the equilibrium structure into the geometry in the complex lies between 0.1 and 0.3 kcal/mol. They are not listed in Table 4. A relatively large Pauli repulsion ΔE_{Pauli} between $M(CO)_5$ and the noble gases in the range of 10 −20 kcal/mol is calculated. The Pauli repulsion is compensated by the electrostatic term

(56) Cremer, D.; Kraka, E. *Angew. Chem.* **1984**, 96, 612; *Angew. Chem., Int. Ed. Engl.* **1984**, *23*, 627.

(57) Thompson, C. A.; Andrews, L. *J. Am. Chem. Soc.* **1994**, *116*, 423.

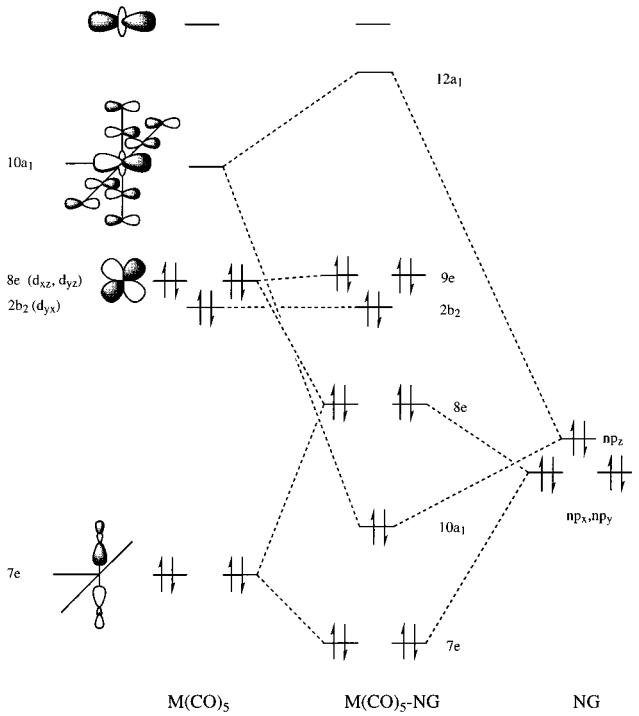

Figure 4. Orbital interaction diagram.

ΔE_{Elstat} and the orbital interactions ΔE_{oi}, leading to an overall attraction between transition metal pentacarbonyl and the noble gas. ΔE_{Pauli} and ΔE_{Elstat} of the chromium and molybdenum complexes have the same order of magnitude and are smaller than those of the tungsten complexes. All interactions increase in the order Ar < Kr < Xe.

The question we now have to answer is which electrons cause these interactions. Demuynck et al.[7] assigned these interactions to the mixing of the metal d orbitals with the noble gas p orbitals, i.e., a destabilizing four-electron interaction of e symmetry between the occupied orbitals np_x and np_y of the noble gas and the occupied orbitals d_{xz} and d_{yz} of the complex and a stabilizing two-electron interaction between the empty d_{z^2} orbital and the occupied np_z Ng orbital. However, our analysis gives a different picture, which is schematically shown in Figure 4. The noble gas np orbitals interact mainly with energetically low lying fragment orbitals of the pentacarbonyl complexes. The transition metal d orbitals are almost unaffected.

Since we build up the wavefunction of the complexes from the converged wavefunctions of the fragments, we can easily extract from our calculation, which orbitals mix with each other. We present in Table 5 the character and energy levels (eV) of the highest occupied (HOMO) and the lowest unoccupied (LUMO) orbitals of $M(CO)_5$ and the $M(CO)_5$-Ng complexes. The d_{xz} and d_{yz} orbitals have their major contribution in the 8e orbital of $M(CO)_5$. As it can be seen from Table 5, the character of the HOMO of the noble gas complexes is pure 8e ($M(CO)_5$). Almost no mixing with the noble gas orbitals takes place, and the orbital levels stay almost unchanged. The reason is that the energy levels of the noble gas np orbitals are too low (e = −10 .3 eV for Ar, −9.3 eV for Kr, and −8.3 eV for Xe) and the ovlerlap $\langle 8e|np_{x,y}\rangle$ is too small.

As a matter of fact, there is a repulsive four-electron interaction of the $np_{x,y}$ orbitals with low-lying pentacarbonyl fragment orbitals of e symmetry. In the case of Ng = Xe, mixing takes place with the 7e orbital (Figure 4) , which is the CO 5σ-based HOMO-2 of $M(CO)_5$. For Kr and Ar, even lower orbitals with CO 1π character are involved. This mixing is, together with the destabilizing interaction of the np_z orbital with appropriate pentacarbonyl fragment orbitals of a_1 symmetry (not shown in Figure 4), responsible for the Pauli repulsion ΔE_{Pauli} (Table 4).

Table 5. Characters and Energies (eV) of HOMO and LUMO of $M(CO)_5$−Ng As Calculated by DFT and Calculated and Experimental[1] $E \rightarrow {}^1A_1$ Excitation Energies (nm)

	$Cr(CO)_5$	$Cr(CO)_5Ar$	$Cr(CO)_5Kr$	$Cr(CO)_5Xe$
ϵ(HOMO)	−6.28	−6.15	−6.08	−6.06
% 8e $(MCO)_5$)	100	99.5	99.0	98.5
$\langle 8e\|np_{x,y}\rangle$		0.05	0.06	0.06
ϵ(LUMO)	−4.63	−4.07	−3.96	−3.87
% np_z (NG)	0	2.8	4.1	5.4
$\langle 10a_1\|np_z\rangle$		0.19	0.21	0.25
$^1E \rightarrow {}^1A_1$	653	523 (533)	516 (518)	504 (492)
	$Mo(CO)_5$	$Mo(CO)_5Ar$	$Mo(CO)_5Kr$	$Mo(CO)_5Xe$
ϵ(HOMO)	−6.28	−6.02	−6.00	−5.94
% 8e $(MCO)_5$)	100	99.9	99.4	98.5
$\langle 8e\|np_{x,y}\rangle$		0.06	0.07	0.08
ϵ(LUMO)	−4.26	−3.64	−3.55	−3.39
% np_z (NG)	0	1.6	2.3	3.0
$\langle 10a_1\|np_z\rangle$		0.20	0.22	0.26
$^1E \rightarrow {}^1A_1$	540	465 (429)	456	442 (413)
	$W(CO)_5$	$W(CO)_5Ar$	$W(CO)_5Kr$	$W(CO)_5Xe$
ϵ(HOMO)	−6.05	−5.92	−5.83	−5.79
% 8e $(MCO)_5$)	100	99.6	99.0	98.0
$\langle 8e\|np_{x,y}\rangle$		0.06	0.07	0.08
ϵ(LUMO)	−4.21	−3.70	−3.48	−3.33
% np_z (NG)	0	2.3	3.2	4.2
$\langle 10a_1\|np_z\rangle$		0.21	0.24	0.28
$^1E \rightarrow {}^1A_1$	576	485 (437)	470	447 (417)

In the case of a_1 symmetry, the stabilizing orbital interaction results mainly from the mixing of the np_z orbital of the noble gas with the $10a_1$ LUMO of $M(CO)_5$. As can be seen from Table 5, the value of the overlap integral $\langle 10a_1|np_z\rangle$ increases in the order Cr < Mo < W and Ar < Kr < Xe, leading to the given trend of increasing $\Delta E_{\text{oi}}(a_1)$ (Table 4). In addition, a small stabilizing orbital interaction due to polarization of the e-type orbitals is found giving a contribution of 2−3 kcal/mol to the bond energy.

The characterization of $10a_1$ as the transition metal d_{z^2} orbital suggested by Demuynck et al. is insufficient. The contribution of the d_{z^2} orbital to the $10a_1$ LUMO of $M(CO)_5$ is very small: 25% in the case of Cr(CO)5 and only 15% for $Mo(CO)_5$ and $W(CO)_5$. In fact, this fragment orbital is dominated by the 2π* orbitals of the equatorial CO and the empty p_z orbital of the transition metal. The metal d_{z^2} orbital itself has its major contribution to the $11a_1$ orbital of $M(CO)_5$, which is the energetically high lying LUMO+3.[58] It is the high contribution of the COeq 2π* orbitals and the emty p_z orbital of the transition metal that is responsible for the high amplitude of the LUMO at the vacant site of $M(CO)_5$ and thus for the efficient overlap with the noble gas p_z orbital.

This becomes also important for the understanding of the sensitivity of the UV spectra on the noble gas. The experimentally observed UV band corresponds to

(58) Rosa, A.; Ricciardi, G.; Baerends, E. J.; Stufkens, D. J. *Inorg. Chem.* **1995**, *34*, 3425.

the $^1E \rightarrow {}^1a_1$ ($b_2^2e^4a_1^0 \rightarrow b_2^2e^3a_1^1$) excitation.[1] We have seen that the energy level of the 9e orbitals of the noble gas complexes are roughly the same for Ng = Ar, Kr, and Xe. That means that the energy difference between 9e HOMO and $12a_1$ LUMO of $M(CO)_5$-Ng depends mainly on destabilization of the $12a_1$ orbital due to the interaction of the noble gas p_z orbital and the LUMO (CO_{ax} hybrid) of $M(CO)_5$ and thus on the overlap $\langle 10a_1 | np_z \rangle$.

We have calculated the $^1E \rightarrow {}^1A_1$ ($e^4a_1^0 \rightarrow e^3a_1^1$) excitation energies using the time-dependent DFT method.[18−21] These values are compared to the experimental excitation energies in Table 5. The agreement between theoretically predicted and experimentally observed excitation energies is excellent. For the chromium complexes $Cr(CO)_5$-Ng, the calculated excitation energies are 523, 516, and 504 nm for Ng = Ar, Kr, and Xe, while the experimental observed UV bands have their maxima at 533, 518, and 492 nm, respectively. The differences between experimentally and theoretically derived excitation energies are somewhat larger (30−50 nm) for the molybdenum and tungsten complexes than for those of chromium.

Since the main stabilizing interaction is due to the overlap between the $M(CO)_5$ 10 a_1 and the NG p_z orbital, it could be argued that a bond angle α larger than 90° should be favored. In fact, when the calculation of Cr-(CO)5-Ar is carried out with α = 95°, this stabilization increases by 0.6 kcal/mol due to a slightly better overlap. On the other side, the repulsive term due to the interaction of the occupied orbitals of both fragments increases by 2 kcal/mol and the stabilization is overcompensated.

Conclusions

The weak interactions between the unsatured 16 e^- fragments $M(CO)_5$ (M = Cr, Mo, W) and the noble gases Ar, Kr, and Xe are well described by ab initio and DFT methods, but the HF-based methods show the typical weakness for calculating first-row transition metals with partly filled d shells. The DFT-based results using various GGAs are in very good agreement with ab initio results using ECPs. The influence of the noble gas on the geometry of the pentacarbonyl is negligible. No significant influence of the kind of the noble gas on the bond angle α between the axial and equatorial carbonyl groups is found. The bond energies predicted using the revised gradient corrections of PW91 are slighly higher than those calculated with BP86. The theoretical bond energies show an increasing trend for the metals Cr < Mo < W and for the noble gases Ar < Kr < Xe. The BSSE-corrected CCSD(T) calculations overestimate the bond strength of the Cr compounds, which leads to the incorrect sequence Mo < Cr < W. The calculations show that DFT methods may be used for weak transition metal−ligand interactions. The interaction of the noble gas with $M(CO)_5$ is dominated by the orbital interactions between the noble gas p orbitals and the orbitals of the equatorial carbonyl groups. The resulting stabilization of the noble gas p_z orbital and the dipole-induced dipole interaction are responsible for the bond between the pentacarbonyl fragments and the noble gases.

Acknowledgment. This work has financially been supported by the Deutsche Forschungsgemeinschaft (SFB 280) and the Fonds der Chemischen Industrie. We thank Dr. Jürgen Gauss for a copy of the program ACES II and Prof. Reinhart Ahlrichs for a copy of the program TURBOMOLE. Excellent service by the HRZ of the Philipps-Universität Marburg and the computanional center SARA and by the foundation Nationale Computer Faciliteiten (NCF) of the Netherlands Foundation for Scientific Research (NWO) are gratefully acknowledged. Additional computer time was provided by the HLRZ Jülich. We also thank the HHLRZ Darmstadt for their support.

OM9704962